Temperature dependence of the band-band absorption coefficient in crystalline silicon from photoluminescence

Hieu T. Nguyen,[1,a)] Fiacre E. Rougieux,[1] Bernhard Mitchell,[2] and Daniel Macdonald[1]
[1]*Research School of Engineering, College of Engineering and Computer Science, The Australian National University, Canberra, ACT 0200, Australia*
[2]*Australian Centre for Advanced Photovoltaics, School of Photovoltaic and Renewable Energy Engineering, University of New South Wales, Sydney, NSW 2052, Australia*

(Received 14 November 2013; accepted 9 January 2014; published online 27 January 2014)

The band-band absorption coefficient in crystalline silicon has been determined using spectral photoluminescence measurements across the wavelength range of 990–1300 nm, and a parameterization of the temperature dependence has been established to allow interpolation of accurate values of the absorption coefficient for any temperature between 170 and 363 K. Band-band absorption coefficient measurements across a temperature range of 78–363 K are found to match well with previous results from MacFarlane *et al.* [Phys. Rev. **111**, 1245 (1958)], and are extended to significantly longer wavelengths. In addition, we report the band-band absorption coefficient across the temperature range from 270–350 K with 10 K intervals, a range in which most practical silicon based devices operate, and for which there are only sparse data available at present. Moreover, the absorption coefficient is shown to vary by up to 50% for every 10 K increment around room temperature. Furthermore, the likely origins of the differences among the absorption coefficient of several commonly referenced works by Green [Sol. Energy Mater. Sol. Cells **92**, 1305 (2008)], Daub and Würfel [Phys. Rev. Lett. **74**, 1020 (1995)], and MacFarlane *et al.* [Phys. Rev. **111**, 1245 (1958)] are discussed. © *2014 AIP Publishing LLC*. [http://dx.doi.org/10.1063/1.4862912]

I. INTRODUCTION

Numerous experimental studies[1–7] have reported measurements of the band-band absorption coefficient in crystalline silicon in the wavelength range near the energy band-gap. Among them, MacFarlane *et al.*[1] used the transmission and reflection characteristics of silicon to establish data at different temperatures, but in a relatively limited wavelength range. Weakliem and Redfield[2] applied the same method but with elevated temperatures up to 475 K and down to wavelengths as small as 460 nm. Green and Keevers,[3] later updated by Green,[4] and Daub and Würfel[6] produced their data independently at 300 K and 295 K, respectively, with a broader wavelength range compared with MacFarlane *et al.* These latter data sets are commonly used today although there is some deviation between them. Green[4] extracted the data from both the transmission and reflection method and the spectral response of high-efficiency silicon solar cells[3–5] while Daub and Würfel[6] analyzed photoluminescence (PL) spectra emitted from optically excited silicon. Later, Trupke *et al.*[7] again utilized this PL-based method to extract data at temperatures covered in the experiment of Ref. 1, but for longer wavelengths.

Recently, there have been some new applications[8,9] relating to silicon solar cells based on fitting photoluminescence spectra. Schinke *et al.*[8] modeled the emitted spectra for silicon wafers with different surface geometries, while Mitchell *et al.*[9] extracted the bulk lifetime of minority carriers in silicon bricks using a fitting of the full PL spectra. These techniques require the band-band absorption coefficient as a key input parameter. They were carried out at 295 K, and both found that the spectra could be fitted better with Daub and Würfel's data (Ref. 6) rather than Green's (Ref. 4). There is significant disagreement in these data sets at wavelengths between 1180–1250 nm, a region which is important for the fitting procedures of the techniques above. However, to date there has been no direct reassessment of the band-band absorption coefficient in order to verify the data at these wavelengths and at this temperature. Moreover, temperatures in experiments of MacFarlane *et al.* and Trupke *et al.* do not densely cover the range in which practical solar cells and microelectronic devices usually operate, and thus there is still a lack of information on the band-band absorption coefficient in crystalline silicon.

The PL-based approach has been demonstrated to have some advantages over the conventional reflection and transmission approach. Previous works[6,7] have shown that it is possible to determine values of the band-band absorption coefficient as low as $10^{-7}\,\mathrm{cm}^{-1}$ at room temperature (RT) via PL measurements, courtesy of the direct relationship between the band-band absorption and emission processes.[11–13] Such sensitivity is not possible with the reflection and transmission method, since impractically thick samples would be required. In any case, free carrier absorption would mask the band-band absorption processes at longer wavelengths in such a transmission experiment,[7] while PL-based data are largely unaffected by free carrier absorption.[10] Therefore, in this study, we again take advantage of this PL-based technique to empirically determine the band-band absorption coefficient in crystalline silicon. First, we perform the measurements at different temperatures and establish a tabulated data set from 78–363 K, especially in the range from 270–350 K with a step of 10 K,

a)Author to whom correspondence should be addressed. Electronic mail: hieu.nguyen@anu.edu.au.

which covers the typical operation temperature of silicon based devices. Next, we investigate the impact of temperature in this temperature range around RT on the band-band absorption coefficient. In addition, we provide a parameterization of the temperature dependence of the absorption coefficient for wavelengths from 990–1300 nm, from which values can be calculated for any temperature between 170 and 363 K. Furthermore, we elucidate the inconsistencies of the absorption data among MacFarlane *et al.*,[1] Daub and Würfel,[6] and Green.[4] Finally, we extend the data up to the wavelength of 1500 nm at 297 K.

II. THEORY AND METHOD

The spontaneous generation rate of photons per volume and energy interval due to band-band transitions in an excited non-degenerate semiconductor is described by the generalized Planck law[11–13]

$$dr_{sp} = C(\hbar\omega)^2 \alpha_{BB}(\hbar\omega)\exp\left(\frac{-\hbar\omega}{kT}\right)\exp\left(\frac{\Delta\eta}{kT}\right)d(\hbar\omega), \quad (1)$$

with $\alpha_{BB}(\hbar\omega)$ the band-band absorption coefficient, k Boltzmann's constant, and T the absolute temperature of the sample. C is given by $n^2/(\pi^2\hbar^3c_0^2)$, with n the refractive index of silicon and c_0 the speed of light in vacuum. As measured in Ref. 14, the refractive index varies approximately 0.5% for every 100 nm wavelength increment around the band-gap, and less than 0.03% for every 10 K increment. Hence, C is usually considered as a constant in Eq. (1). $\Delta\eta$ is the difference between the quasi-Fermi levels of electrons and holes under illumination. Since $\Delta\eta$ is independent of wavelength, the $\exp(\Delta\eta/kT)$ factor is also a constant for a fixed injection level at a particular temperature.

To obtain the total photon flux outside the sample, one has to integrate Eq. (1) over its thickness and account for the reabsorption of emitted photons within it. For planar samples excited by monochromatic light, the photon flux, in this case called the PL signal, emitted outside these samples per energy interval is given by[6,7,10,11]

$$PL = \frac{dr_{sp}A(\hbar\omega)}{4\alpha_{BB}n^2} = \frac{1}{4\pi^2\hbar^3c_0^2}(\hbar\omega)^2 A(\hbar\omega)\exp\left(\frac{-\hbar\omega}{kT}\right)\exp\left(\frac{\Delta\eta}{kT}\right)d(\hbar\omega), \quad (2)$$

with $A(\hbar\omega)$ the absorptivity at a given energy, which is approximated via the following formula after multiple incoherent reflections between two surfaces are included[6,7,10,11]

$$A(\hbar\omega) = \frac{[1-R_f(\hbar\omega)][1-e^{-\alpha_{BB}(\hbar\omega)d}][1+R_b(\hbar\omega)e^{-\alpha_{BB}(\hbar\omega)d}]}{1-R_f(\hbar\omega)R_b(\hbar\omega)e^{-2\alpha_{BB}(\hbar\omega)d}}, \quad (3)$$

with d the sample thickness, R_f and R_b the reflectivity of the front and back surfaces relative to the illuminated side. As simulated with the OPAL optical simulator developed by McIntosh and Baker-Finch[15,16] at wavelengths 1100 and 1200 nm, the internal reflectivity of emitted luminescence at the silicon/SiN/air interface varies less than 10% relative for incident angles less than the critical angle for the sample investigated in this study. Based on this modeling, we conclude that the internal reflectivity is effectively independent of the angle of incidence for rays that contribute to the PL signal, and equal to the externally measured reflectance for a normally incident beam.

In order for Eqs. (2) and (3) to be valid, the charge carrier profile must be homogeneous through the sample thickness, and the reabsorption of emitted photons is assumed to be dominated by the band-band absorption,[6,7] rather than other processes such as free carrier absorption. The first point is true for samples whose diffusion lengths are several times larger than their thicknesses, while the second assumption was justified by Trupke *et al.*[10] for wavelengths below 1300 nm for silicon wafers with standard background doping levels in solar cell applications, in which the free carrier density is less than $2 \times 10^{17}\,\mathrm{cm}^{-3}$.

An advantage of this photoluminescence technique is that one can avoid the need to measure the absolute values of PL spectra, which is difficult in practice. The PL signal is instead measured in relative units using an optical spectrometer, from which the relative absorptivity is calculated by dividing the PL signal by the $(\hbar\omega)^2\exp(-\hbar\omega/kT)$ term, in accordance with Eq. (2). A scaling factor is then obtained from one absolute value of the absorptivity, calculated from Eq. (3) together with one literature value of α_{BB} from Ref. 1 at 1065 nm (for 78 and 90 K) or 1110 nm (for other temperatures), and the relative one. The reason for choosing these two wavelengths will be explained in Sec. IV A. This scaling factor is used to convert all relative data of the absorptivity into absolute data. Finally, Eq. (3) is solved to acquire α_{BB} for all wavelengths.

Note that further reference to the absorption coefficient in this paper refers to band-band transitions only.

III. EXPERIMENTAL DETAILS

Figure 1 shows the schematic of our experiment. Our sample was illuminated from the front by a mechanically chopped monochromatic laser diode, and the emitted PL signal was detected from the same side. The laser beam was perpendicular to the sample surface. The laser had a wavelength of 785 nm, on-sample power of 250 mW, and beam diameter of 2.2 mm. The emitted signal was focused onto the entrance port of a double-grating monochromator with blazed gratings of 600 grooves/mm and 1000 nm blaze by a

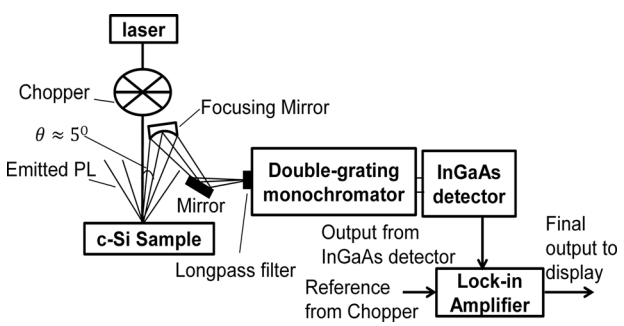

FIG. 1. Schematic of the photoluminescence spectroscopy system used to capture the PL spectra emitted from silicon.

focusing mirror whose central point, along with the illuminated spot, created an angle of about 5° relative to the laser beam (this angle is denoted by θ in Figure 1). The signal was then captured by a liquid-nitrogen-cooled InGaAs detector with a 1 mm^2 active area. The detector output, along with a reference signal from the optical chopper, was fed into a digital lock-in amplifier where the PL spectrum was measured with a modulation frequency of 500 Hz. The final output was connected to a pre-amplifier before being displayed by a computer. A long-pass filter was located in front of the monochromator to avoid the laser light being reflected directly towards the detector. A liquid-nitrogen-cooled cryostat was used to control the sample temperature precisely from 78 to 363 K. The spectra were measured at wavelength intervals of 5 nm and a typical integration time of 10 s. The slit width was adjusted to allow a wavelength integration interval of 5 nm for each data point.

The investigated silicon sample was a high quality phosphorus-doped n-type float zone wafer, 220 μm thick, whose two sides were chemically polished to achieve planar surfaces. The resistivity was 3 Ω cm, corresponding to a background doping level of 1.6×10^{15} cm^{-3}. Both surfaces were passivated by a 75 nm thick layer of silicon nitride (SiN) deposited by plasma-enhanced chemical-vapor deposition (PECVD). The external reflectivity of both sides was measured accurately by a spectrophotometer with a built-in 150 mm integrating sphere and automated reflectance and transmittance analyzer. Before the PL measurement, the sample was irradiated for two hours and the temperature was monitored with a thermocouple mounted behind the illuminated spot. The temperature increased less than 1.5 K, allowing us to neglect the heating effect on the illuminated spot.

Under the high injection conditions that prevail during the PL measurements in this study, the passivation quality of the SiN films may be quantified via the so-called emitter saturation current density J_{Oe}.[17] This quantity was measured with the transient photo-conductance decay technique[18] under high injection, and was found to have a value of 11 fA/cm^2 for both sides combined. Typically, this parameter is used to characterize the surface recombination associated with diffused layers, however, it is also applicable to surfaces under high injection passivated by dielectric films with high fixed charge densities, such as the SiN films used here. The fixed charge induces a charge separation layer just below the surface, which acts in a similar manner to a diffused region in terms of recombination. From this value of the saturation current density, the carrier profile as a function of depth was simulated with the simulation spreadsheet developed by Cuevas.[19,20] Klaassen's mobility model[21,22] was used to estimate the carrier mobilities in this simulation, and the Auger lifetime was estimated via the model of Kerr and Cuevas.[23] The laser has an average intensity of 60 suns and a spatial Gaussian distribution. The simulation was carried out under a generation rate of 120 suns, which is equivalent to the peak intensity of the laser at the center of the illuminated spot.

Figure 2 shows the simulated excess carrier profile at the center of the illuminated spot through the thickness of the investigated wafer at RT. The difference between the front and back surfaces is less than 15%, indicating an almost uniform carrier distribution. Outside this central point, the minority carrier lifetime, and therefore the diffusion length, will be even larger, due to the lower local injection level, thus the carrier profile will be more uniform than the center. Therefore the conditions for which Eq. (2) is valid are fulfilled. At other temperatures, we assume that no significant non-uniformities arise in the carrier profile, which we find justified by the very good agreement with the data of MacFarlane *et al.*, as shown below.

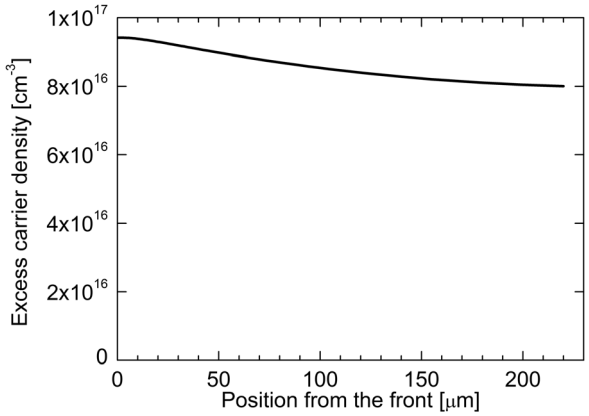

FIG. 2. Simulated excess carrier profile at the center of the illuminated spot at RT.

IV. RESULTS

A. Temperatures in the experiment of MacFarlane *et al.*

With the temperature controlled precisely (varied less than 0.5 K) by a liquid-nitrogen-cooled cryostat, PL spectra were captured at the same temperatures covered in the experiment of MacFarlane *et al.*[1] This was done in order to verify the accuracy of our data across a range of temperatures, and also to extend the data of MacFarlane *et al.* to longer wavelengths.

The resulting normalized PL spectra are shown in Figure 3. The spectra clearly show two fundamental characteristics of silicon luminescence. The first is the band-gap

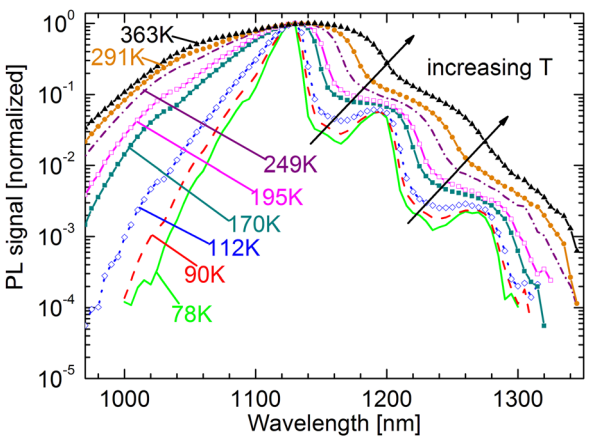

FIG. 3. PL spectra captured at temperatures covered in the experiment of MacFarlane *et al.*

widening effect at low temperature.[24] The band-band peak at the highest point of the spectrum is shifted toward shorter wavelength side, i.e., higher energy, when the temperature decreases from 363 down to 78 K. The second feature is the evolution of the phonon edges with temperature. In figure, three shoulders in each spectrum can be observed for each temperature, and these become more distinguishable at lower temperatures. These three shoulders, starting from left to right, correspond to photon emission mediated by the concomitant emission of one-, two-, and three-phonons, respectively. Since the density of phonons is reduced and their energy distribution is narrowed at low temperatures,[25] the shoulders become sharper and more distinct as the temperature is reduced. Due to the widening of the band-gap, these shoulders also move to higher energies at lower temperatures. A shoulder corresponding to photon emission mediated by single-phonon absorption can also be observed at wavelengths around 1050 nm at high temperatures.

These spectra, along with digitized values of the absorption coefficient from MacFarlane *et al.*[1] at 1065 nm for 78 and 90 K and at 1110 nm for other temperatures, were used to extract the absorption coefficient values for wavelengths from 990–1300 nm. The first wavelength at 1065 nm was chosen to avoid the very sharp transition of the band-band peak at low temperatures, while the second wavelength at 1110 nm was selected to avoid the phonon edges where the temperature uncertainty had a larger impact at higher temperatures. Also note that Ref. 1 represented the data in terms of the square root of the product of the energy and the absorption coefficient versus the energy (see Figure 1 in Ref. 1). In this work, we have converted these values into the absorption coefficient.

Figure 4 plots our data and the data of Ref. 1. The data sets agree very well, except for a small variation at high wavelengths around 1150 nm. At these wavelengths, the values of the absorption coefficient are on the order of $1\times10^{-3}\,\mathrm{cm}^{-1}$, which is difficult to measure precisely by the conventional transmission and reflection approach. Meanwhile, the band-band peak of the PL spectrum is located around 1150 nm, where the signal-to-noise ratio in our PL measurements is larger than 10^3, as depicted in Figure 5, giving a small measurement uncertainty. In addition, given the linear axis used in the plot of MacFarlane *et al.*,[1] there is an increasing amount of digitization error when extracting data at these low values of the absorption coefficient. Finally, the very good agreement evidently validates our assumption of homogeneous carrier profiles at the various temperatures studied.

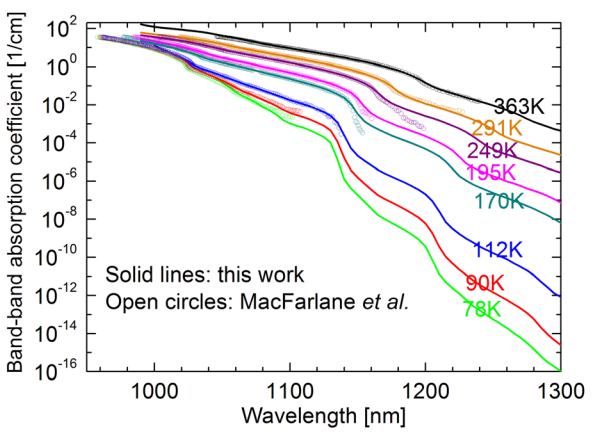

FIG. 4. Absorption coefficient in crystalline silicon obtained from PL at different temperatures 78, 90, 112, 170, 195, 249, 291, and 363 K in this work (solid lines) in comparison with MacFarlane *et al.* (open circles).

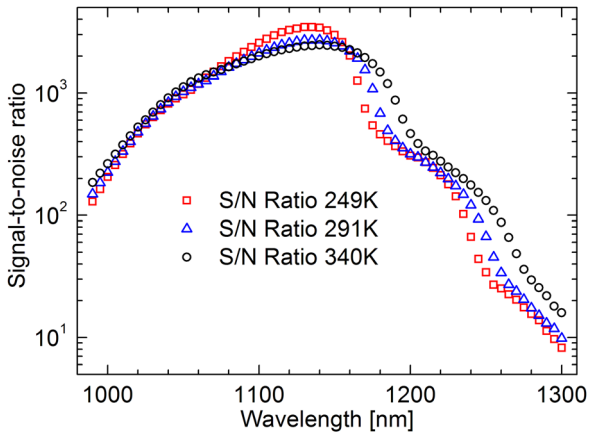

FIG. 5. Signal-to-noise ratio of PL spectra around RT. The data were obtained by subtracting the average background noise from the PL signal, then dividing the results by two standard deviations of the background noise.

B. Temperatures around RT

With the very good agreement with the data of MacFarlane *et al.*, we extended our measurements to different temperatures which were not covered in their experiment. The PL spectra are plotted in Figure 6. These temperatures, from 270 to 350 K, cover a more practical operation range for silicon based devices.

In Figure 7, we have plotted values of the absorption coefficient extracted from Ref. 1 at 1110 nm (1.117 eV) versus temperature, and then fitted these points with a 6th order polynomial. From this function, we interpolated values at other temperatures near RT. These values, along with the spectra in Figure 6, were used to calculate the absorption coefficient data at temperatures between 270 and 350 K at 10 K intervals, which are presented in Figure 8. These data may be useful for modeling the operation of working devices such as solar cells. The data at 297 K are also presented here

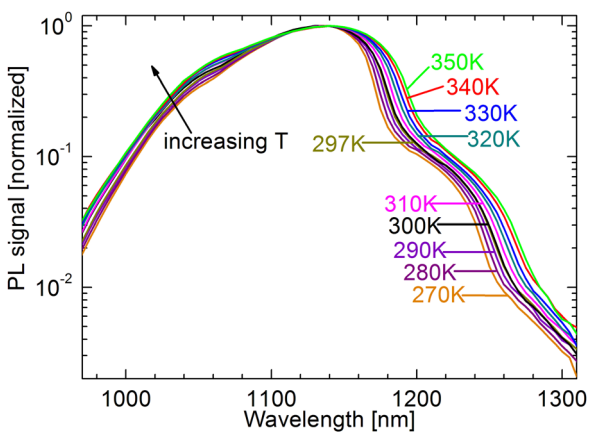

FIG. 6. PL spectra at temperatures near RT, from 270–350 K.

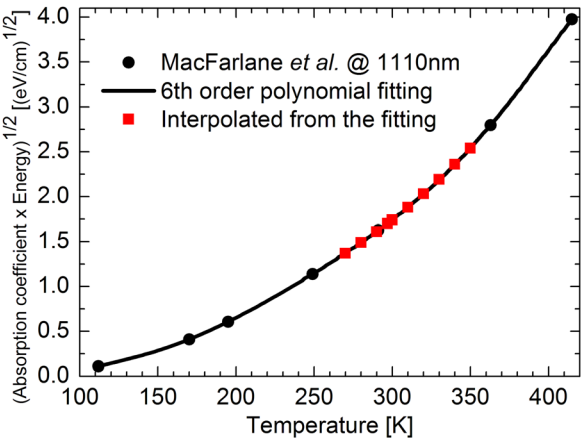

FIG. 7. 6th order polynomial fitting (solid line) for the data of MacFarlane *et al*. (black circles) of the absorption coefficient at wavelength 1110 nm, or energy 1.117 eV. From this fitting, values at temperatures between 270 and 350 K were interpolated (red squares).

since this temperature is often considered to be room temperature.

Further, we have calculated the relative change of the absorption coefficient for several 10 K increments around RT. The results, plotted in Figure 9, show that the variation is mostly less than 20% for wavelengths between 990 and 1150 nm, but increases up to 50% and above for wavelengths between 1200 and 1300 nm. Therefore, we conclude that relatively small changes in temperature can significantly impact the band-band absorption coefficient in crystalline silicon.

C. Parameterization of the temperature dependence

With the dense intervals of temperatures and wavelengths in our experiments, we can establish an accurate temperature-dependent parameterization of the absorption coefficient. For each wavelength, we used the values from six different temperatures 170, 195, 249, 291, 310, and 363 K to build a 5th order polynomial fitting function, which had the form of $\sum_{i=0}^{5} a_i T^i$. The coefficients a_i of this polynomial are called the temperature coefficients in this work, from which the data at other temperatures can be interpolated. Figure 10 shows our reconstructed data using these

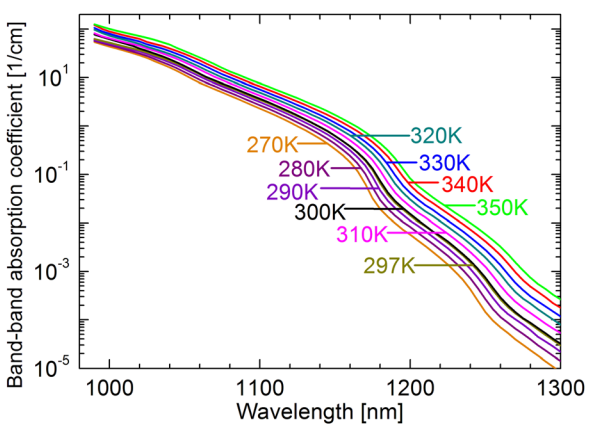

FIG. 8. Absorption coefficient of silicon obtained from PL at temperatures between 270 and 350 K. The data at 297 K and 300 K are almost overlapping.

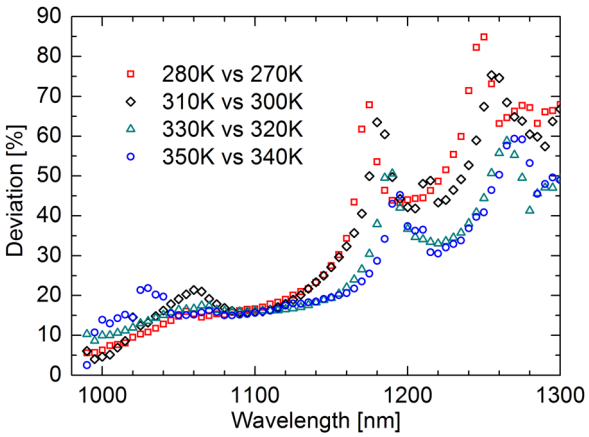

FIG. 9. Relative increment of the absorption coefficient for every 10 K increment around RT.

coefficients from this fitting method compared with experimental data at some intermediate temperatures. The data sets are in excellent agreement. With these temperature-dependent parameters, one can interpolate the values of the absorption coefficient at any given temperature between 170 and 363 K for wavelengths from 990–1300 nm.

The advantage of our method is that it is based on interpolation of relatively dense data. By comparison, Green[4] obtained the temperature coefficients for wavelengths above 840 nm by extrapolating data from Ref. 26, in which the experiments were performed for wavelengths below 840 nm. Also note that this extrapolation misses the details of the temperature dependence of changes in band-gap energy, the shift of phonon edges, and the broadening of phonon distributions when the temperature increases. Our experiments allow the changes in those features with temperature to be revealed clearly in the spectra, and are accurately described by the interpolation method.

D. Comparison with independently measured spectra

As an additional verification of the accuracy of our absorption coefficient data, we reproduce the full PL spectrum fitting demonstrated in Mitchell *et al*.[9] on a 5 in. thick monocrystalline Cz-grown silicon brick (see Ref. 9 for the

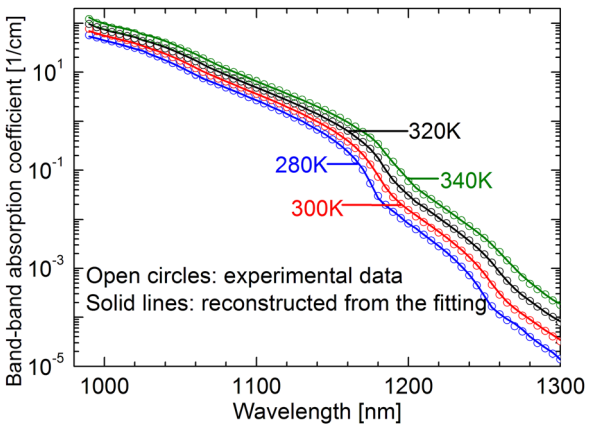

FIG. 10. Comparison of the absorption coefficient from this work between the experimental data and the reconstructed data using the 5th order polynomial fitting.

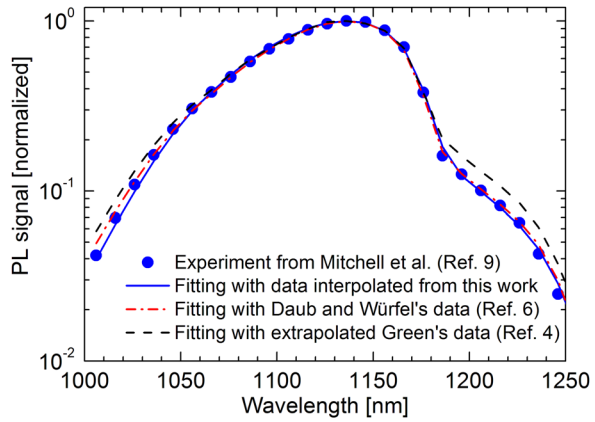

FIG. 11. Experimental PL spectrum of silicon brick from Mitchell *et al.* with theoretical fit using our interpolated absorption coefficient at 295 K as the input parameter. Fits using the data of Daub and Würfel, and Green are also shown here for comparison.

full fitting procedure). The absorption coefficient is a key input parameter in the fitting of the theoretical spectrum, as proposed by Green.[27] Mitchell *et al.* used the absorption coefficient data published by Daub and Würfel[6] and Green[4] to fit the brick measurement (see Figure 9 in Ref. 9). Here, we reproduce this graph, but also include the fit using our absorption data at 295 K as the input for Green's formula. We employed the interpolation procedure described above to obtain values at 295 K.

The spectral PL measurement carried out by Mitchell *et al.* varies from the one used in this study, for example, in the laser wavelength and power, the size of the illuminated spot, and the type of monochromator. Importantly, the sample used by Mitchell *et al.* is an unpassivated silicon brick rather than a thin and passivated silicon wafer as in our study. Despite these differences in the experimental approach, our data give excellent agreement with the measured spectrum in Mitchell *et al.*, as shown in Figure 11.

We note that in Figure 11, the fit using Green's data is 30% higher than the experimental spectrum at wavelengths around 1200 nm, while the two fits using Daub and Würfel's, and our data are almost identical to the experiment. This variation will be clarified in the Sec. IV E.

E. Comparison of RT absorption coefficient data

We compare and elucidate the inconsistencies of the absorption data at 295 K among some commonly used works. Daub and Würfel's,[6] Green's,[4] and our data are shown in Figure 12 and their relative variations in Figure 13. At 295 K Green's data were exponentially extrapolated using the temperature coefficients from Ref. 4.

In Figure 13, our data are consistently around 15% lower than Daub and Würfel's. This difference could stem from the scaling method to get the absolute absorptivity. Daub and Würfel[6] assumed that the absorptivity was saturated on the high energy side of the spectrum, i.e., $\alpha_{BB}d \gg 1$, and used the absolute value $A = 1–R$, where R is the surface reflectivity, to obtain the scaling factor. However, this is not entirely accurate, since $\alpha_{BB}d \gg 1$, with the authors' sample thickness of 262 μm, would require $\alpha_{BB} \gg 40$ cm^{-1}. However, even at the wavelength of 950 nm, α_{BB} is just 150 cm^{-1} at 295 K (extrapolated from Ref. 4), and does not fully satisfy the saturation condition. Second, the excess carrier density can be slightly reduced at the surface due to imperfect surface passivation. Since on the high energy side, more photons are emitted by a volume near the surface than from deeper inside the sample,[28] this suppressed carrier concentration near the surface may reduce the relative strength of the high energy part of the PL spectrum. Thus, scaling the high energy side to $1–R$ may shift up the entire data set. By comparison, in the experiments of MacFarlane *et al.*,[1] for wavelengths close to the band-gap, such as 1110 nm (1.117 eV) as we have chosen to scale our data, one just needs to measure the reflectance and transmittance, and the sample thickness, to extract the absorption coefficient accurately. The errors in these measurements were estimated to be about 1%,[1,29] thus too small to significantly affect the absorption coefficient. Therefore, we can minimize these possible systematic errors. However, it should also be noted that the experimental uncertainties in both Daub and Würfel's, and our data could also contribute to the differences in Fig 13, in particular at longer wavelengths, where the signal-to-noise ratio for our data decreases to around 10 at 1300 nm, as shown in Figure 5. In a similar way, Daub and

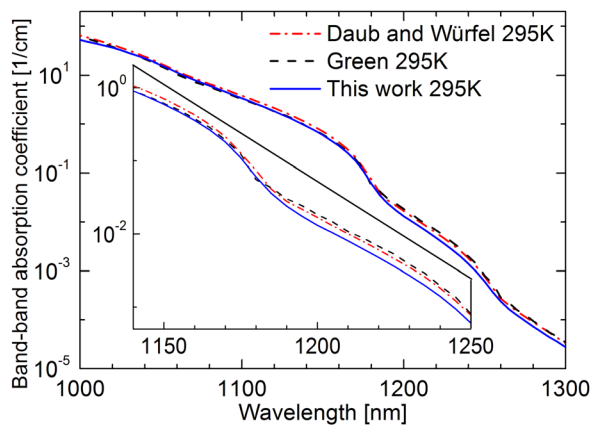

FIG. 12. Absorption data at 295 K. The insert is a zoomed-in section of wavelengths from 1140–1250 nm.

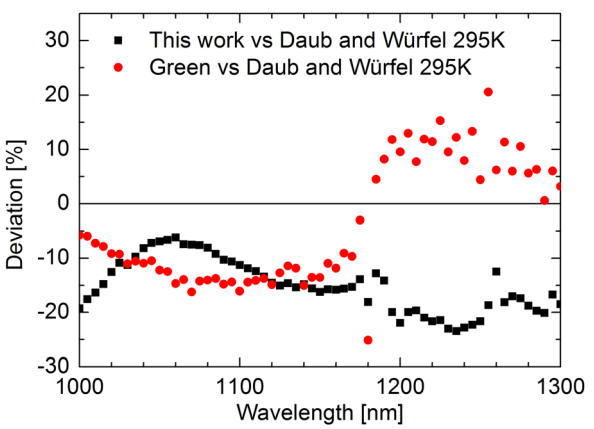

FIG. 13. Quantitative comparison of the absorption data among this work, Green, and Daub and Würfel at 295 K.

Würfel's data must also have been subject to a decreasing signal-to-noise ratio at longer wavelengths.

In addition, Figure 13 also shows that Green's data are 15% lower than Daub and Würfel's for wavelengths below approximately 1170 nm, but increase to 10% higher than Daub and Würfel's for longer wavelengths. Since Schinke *et al.*[8] and Mitchell *et al.*[9] normalized their spectra to the band-band peak around 1150 nm, they saw up to 30% deviation using Green's data at wavelengths around 1200 nm.

Finally, Figure 14 compares the absorption data from this work, Daub and Würfel,[6] and Green[4] with MacFarlane *et al.*[1] at 295 K. The data of MacFarlane *et al.* were interpolated by a 4th order polynomial derived from data at temperatures 195, 249, 291, 363, 415 K from Ref. 1. The wavelength range is limited from 1070–1150 nm where the data used to create the polynomial fitting are available. Green's and this work's values vary less than 6% from MacFarlane *et al.*, as expected since they were scaled to the data of MacFarlane *et al.* Daub and Würfel's data set shows consistently 15% higher values possibly due to the different scaling method used in that work and the uncertainties in the measurements, as described above.

F. Extended wavelengths at 297 K

We have also extended the measurement at 297 K up to the wavelength of 1500 nm. In this experiment, we did not use the cryostat to control the temperature, since the cryostat reduced the PL signal significantly, due to absorption and reflection from the cryostat windows, leaving the signal too noisy to be captured at longer wavelengths. With the cryostat removed, we measured the spectrum in two parts: the first with wavelengths from 950–1310 nm and the second from 1255–1500 nm. Since the residual PL signal of the second half is more than an order of magnitude lower, this section was captured with the maximum gain of the lock-in amplifier, and with an increased integration time of 200 s for each wavelength. The relative spectrum was then scaled down to match the first half, and the two spectra stitched together, while other experimental conditions were kept unchanged. This scaling factor (SF) was swept through a variety of values, for each of which the weighted sum of square error (SSE) was computed for the overlapping part of the two halves by Eq. (4), and then the value giving the least SSE was chosen

$$SSE = \sum_{overlapped} \left(\frac{1st - 2nd \times SF}{1st} \right)^2. \quad (4)$$

With this stitching technique, we were able to extend the data to wavelengths up to 1500 nm. However, we observed a small peak at wavelengths between 1415–1420 nm, denoted by a dotted circle in Figure 15, in all of our measurements for numerous different samples. This unexpected peak was not caused by the laser's second harmonic since its wavelength was 785 nm. Thus, we hypothesize that this peak was a very weak, unidentified optical artifact of our system. Also note that the signal-to-noise ratio was in general improved in these measurements, due to the increased PL signal with the cryostat removed. At 1300 nm, the signal-to-noise ratio was estimated to be 40 compared to around 10 for the cryostat data. However, at 1500 nm, the signal-to-noise ratio decreased further, approaching values around 1, and therefore reaching the sensitivity limit of our experimental setup.

Using the same method as in Secs. IV A and IV B, this spectrum, along with the value of the absorption coefficient at wavelength 1110 nm from MacFarlane *et al.*,[1] was used to scale and compute our data at 297 K. Our data with and without using the cryostat, along with data from Green at 297 K (extrapolated from Ref. 4), and Daub and Würfel[6] at 295 K, are shown in Figure 16 for a qualitative comparison. In the figure, the two data sets with and without using the cryostat are almost identical. This again confirms that the cryostat did not cause any systematic errors in our previous experiments. However, it should also be noted that the data at wavelengths above 1300 nm may be more impacted by free carrier absorption than in the narrower wavelength range presented above.

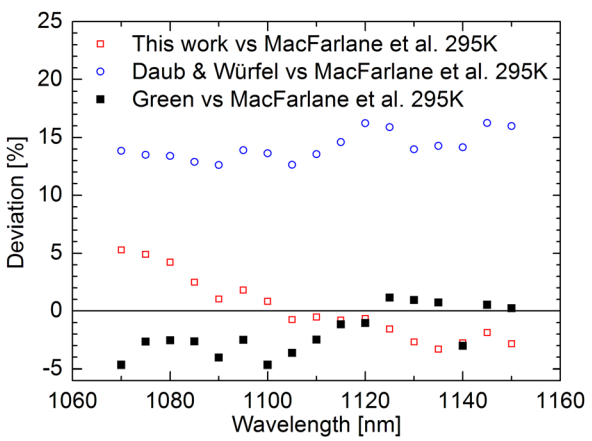

FIG. 14. Quantitative comparison of the absorption data from this work, Daub and Würfel, and Green with MacFarlane *et al.* at 295 K for wavelengths from 1070–1150 nm.

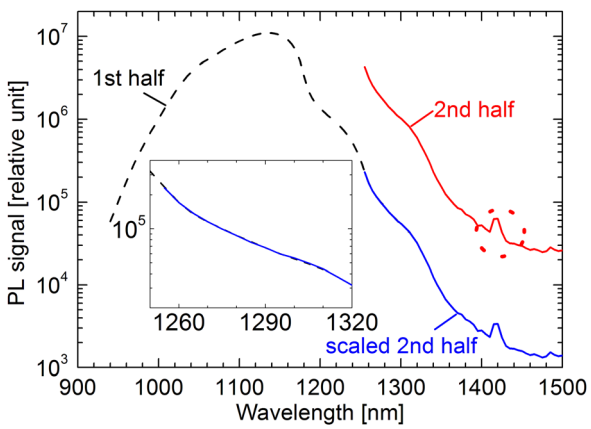

FIG. 15. PL spectrum captured by the stitching method at 297 K without using the cryostat. The second half (red solid) was captured with maximum gain of the lock-in amplifier, which was scaled down (blue solid) to match the first half (black dash). The insert is a zoomed-in section of the overlapping region.

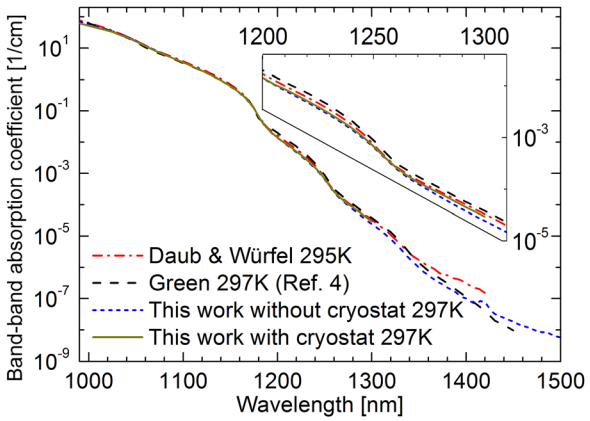

FIG. 16. Comparison of the absorption data at 297 K. Our data with and without cryostat are almost identical. The insert is a zoomed-in section for wavelengths from 1200–1310 nm.

V. CONCLUSIONS

We have presented temperature-dependent data for the band-band absorption coefficient in crystalline silicon, across a wavelength range from 990–1300 nm from spectral photoluminescence measurements, and established a parameterization of the data to allow interpolation of accurate values of the band-band absorption for any temperature between 170 and 363 K. Our data show very good agreement with the data of MacFarlane *et al*. In addition, we have demonstrated the significant impact of temperature on the band-band absorption coefficient near room temperature. Furthermore, we have discussed the possible origins of mismatches among the data sets of MacFarlane *et al*., Green, and Daub and Würfel. Finally, we have extended data up to the wavelength of 1500 nm at 297 K. All data for the absorption coefficient, the temperature-dependence parameters for each wavelength, and the normalized PL spectra are tabulated in the electronic attachment to this paper.[30]

ACKNOWLEDGMENTS

This work has been supported by the Australian Research Council (ARC) and the Australian Renewable Energy Agency (ARENA). The authors thank Di Yan for providing the silicon wafer, Teck Chong for assisting with the reflectivity measurements, Dr. Erich Daub for supplying his absorption coefficient data set, and Dr. Thorsten Trupke for very helpful discussions.

[1]G. G. MacFarlane, T. P. MacLean, J. E. Quarrington, and V. Roberts, Phys. Rev. **111**, 1245 (1958).
[2]H. A. Weakliem and D. Redfield, J. Appl. Phys. **50**, 1491 (1979).
[3]M. A. Green and M. J. Keevers, Prog. Photovoltaics **3**, 189 (1995).
[4]M. A. Green, Sol. Energy Mater. Sol. Cells **92**, 1305 (2008).
[5]M. J. Keevers and M. A. Green, Appl. Phys. Lett. **66**, 174 (1995).
[6]E. Daub and P. Würfel, Phys. Rev. Lett. **74**, 1020 (1995).
[7]T. Trupke, M. A. Green, P. Würfel, P. P. Altermatt, A. Wang, J. Zhao, and R. Corkish, J. Appl. Phys. **94**, 4930 (2003).
[8]C. Schinke, D. Hinken, J. Schmidt, K. Bothe, and R. Brendel, IEEE J. Photovoltaics **3**, 1038 (2013).
[9]B. Mitchell, M. K. Juhl, M. A. Green, and T. Trupke, IEEE J. Photovoltaics. **3**, 962 (2013).
[10]T. Trupke, E. Daub, and P. Würfel, Sol. Energy Mater. Sol. Cells **53**, 103 (1998).
[11]P. Würfel, J. Phys. C **15**, 3967 (1982).
[12]P. Würfel, S. Finkbeiner, and E. Daub, Appl. Phys. A: Mater. Sci. Process. **60**, 67 (1995).
[13]P. Würfel, T. Trupke, T. Puzzer, E. Schäffer, W. Warta, and S. W. Glunz, J. Appl. Phys. **101**, 123110 (2007).
[14]H. W. Icenogle, B. C. Platt, and W. L. Wolfe, Appl. Opt. **15**, 2348 (1976).
[15]K. R. McIntosh and S. C. Baker-Finch, in *Proceedings of the 38th IEEE Photovoltaic Specialists Conference* (2012), p. 265.
[16]S. C. Baker-Finch and K. R. McIntosh, in *Proceedings of the 35th IEEE Photovoltaic Specialists Conference* (2010), p. 2184.
[17]A. Cuevas and D. Macdonald, Sol. Energy **76**, 255 (2004).
[18]D. E. Kane and R. M. Swanson, in *Proceedings of the 18th IEEE Photovoltaic Specialists Conference* (1985), p. 578.
[19]A. Cuevas and R. Sinton, in *Proceedings of the 23rd European Photovoltaic Solar Energy Conference* (2008), p. 315.
[20]A. Cuevas, Energy Procedia **8**, 94 (2011).
[21]D. B. M. Klaassen, Solid-State Electron. **35**, 953 (1992).
[22]D. B. M. Klaassen, Solid-State Electron. **35**, 961 (1992).
[23]M. J. Kerr and A. Cuevas, J. Appl. Phys. **91**, 2473 (2002).
[24]W. Bludau, A. Onton, and W. Heinke, J. Appl. Phys. **45**, 1846 (1974).
[25]H. M. Rosenberg, *The Solid State* (Oxford University Press, New York, 1988), p. 91.
[26]G. E. Jellison, Jr. and F. A. Modine, J. Appl. Phys. **76**, 3758 (1994).
[27]M. A. Green, Appl. Phys. Lett. **99**, 131112 (2011).
[28]T. Trupke, J. Appl. Phys. **100**, 063531 (2006).
[29]G. G. MacFarlane, T. P. MacLean, J. E. Quarrington, and V. Roberts, Phys. Rev. **108**, 1377 (1957).
[30]See supplemental material at http://dx.doi.org/10.1063/1.4862912 for the full tabulated data set.